Morphology-controlled synthesis of $SrTiO_3$ micro-scale particles*

Cao Jia-Feng(曹加锋)† and Ji Yue-Xia(冀月霞)

School of Mathematics and Physics, Anhui University of Technology, Maanshan 243032, *China*

(Received 7 November 2013; revised manuscript received 14 March 2014; published online 10 October 2014)

A novel and simple strategy of morphology-controlled $SrTiO_3$ (ST) micro-scale particle synthesis by the flux method is reported. Systematic experiments are designed to realize the tunable morphologies of the particles when the flux salt, sintering process, and the precursors are changed. The ST plates can be synthesized by plate-like $Bi_4Ti_3O_{12}$ (BIT) precursors in NaCl flux. However, the as-synthesized $Bi_4Ti_3O_{12}$ grains transform into reticular particles and finally into rods at higher temperature in NaCl and KCl compounds. Besides, cubic ST particles are also prepared using different precursors as a comparative experiment. This study provides a strategy for further investigations in designing the morphology-controlled particles and efficient anisotropic materials of perovskite structure such as ferroelectric and photocatalyst.

Keywords: morphology-controlled synthesis, $SrTiO_3$ particles, topochemical microcrystal conversion

PACS: 81.10.–h, 81.05.–t, 81.10.Fq **DOI:** 10.1088/1674-1056/23/12/128104

1. Introduction

Strontium titanate, a famous perovskite material, has been widely studied due to its excellent dielectric, photoelectric, and optical properties.[1–5] Besides, as a promising photocatalytic candidate, $SrTiO_3$ has been widely studied in splitting water into H_2 and O_2 and decomposing organic compounds due to its excellent photocatalytic performance.[6–12] Conventionally, $SrTiO_3$ is synthesized from $SrCO_3$ and TiO_2 powders by a solid state reaction, which results in large particle sizes, low surface areas, and irregular particle morphologies.[13] Compared with the bulk counterparts, specific morphology-controlled structures[14,15] always exhibit physical and chemical properties,[16–18] and much effort has been made to understand the electronic,[19,20] magnetic,[21] and optical properties[22] of these structures. Though it has exhibited good performances compared with the traditional morphology,[23,24] few research results have been systematically reported about the flux synthesis of $SrTiO_3$ with specific grain orientations and different morphologies. On the one hand, many methods have been suggested to overcome the disadvantages synthesized by the conventional process;[11] on the other hand, the topochemical microcrystal conversion (TMC) method has been successfully used to synthesize perovskite-structured template seeds such as $NaNbO_3$,[25] $KNbO_3$,[26] and $Na_{0.5}Bi_{0.5}TiO_3$.[27]

Therefore, in this paper, we use the two-step molten salt method to synthesize $SrTiO_3$ with plate-, reticula-, rod-, and cube-shapes in NaCl and KCl. $Bi_4Ti_3O_{12}$ (BIT) particles are prepared as precursors because of their excellent platelet morphologies in the two-step molten salt method. Different shapes obtained under various processes are analyzed in detail, and it is indicated that the precursors, the flux salt and the sintering processes are the important factors that seriously affect the final morphologies of $SrTiO_3$ particles.

2. Experimental details

2.1. Preparation of plate-like BIT precursors

In order to optimize the morphology of $SrTiO_3$, optimized plate-like intermediate $Bi_4Ti_3O_{12}$ (BIT) with anisotropic properties was first synthesized in this research. Bi_2O_3 and TiO_2 (analytical reagent) were used as the bismuth and titanium precursors with 1-mol% excessive Bi_2O_3. To prepare BIT particles, the raw compounds were mixed with NaCl in a weight ratio of 1:2. The mixture was first heated at 800 °C at a heating rate of 10 °C·min^{-1} for 1 h to melt NaCl and then to 920 °C at a heating rate of 6 °C·min^{-1} for 2 h followed by furnace annealing. For comparison, the compounds of Bi_2O_3, TiO_2, and the same amount of flux (NaCl:KCl = 1:1 in mole ratio) were first heated at 660 °C at the same sintering rate for an hour followed by a higher temperature treatment at 920 °C for 2 h. The final products were washed with diluting water several times to remove NaCl/NaCl–KCl impurities.

2.2. Synthesis of ST-1, ST-2, and ST-3 particles

In our experiments, the plate-like $SrTiO_3$ (denoted as ST-1), reticular ST (denoted as ST-2), and rod-like $SrTiO_3$ (denoted as ST-3) were synthesized by a two-step molten salt method, except for the cubic $SrTiO_3$ particles (denoted as ST-4) which were produced by a single molten salt method. As shown in Fig. 1, ST-1 particles were prepared by BIT plates and $SrCO_3$ in a mole ratio of 1:3. The mixture was homogenized thoroughly with flux salt (NaCl) in a weight ratio of 1:4 and sintered in the furnaces. ST-2 and ST-3 samples were prepared by the same method but the fluxes (1:4 in a weight

*Project supported by the National Natural Science Foundation of China (Grant No. 11404004).

†Corresponding author. E-mail: cjf786@163.com

© 2014 Chinese Physical Society and IOP Publishing Ltd

ratio) were NaCl–KCl compounds (50%-mol NaCl and 50%-mol KCl). The final products were washed by the HNO_3 solution and diluting water several times to remove the impurities. For comparison, the $SrTiO_3$ cubes (ST-4) were first sintered in NaCl–KCl flux (1:4 in weight ratio and NaCl:KCl = 1:1 in mole ratio) from $SrCO_3$ and TiO_2 precursors, and the sample was washed by diluting water to obtain pure products. It should be noted that all the sintering processes in the experiments included a primary flux-melting procedure at low temperature and a rate of 10 °C·min^{-1} for 2 h, a high sintering procedure to reach the aimed points at a rate of 6 °C·min^{-1}, and finally an annealing procedure in the furnace.

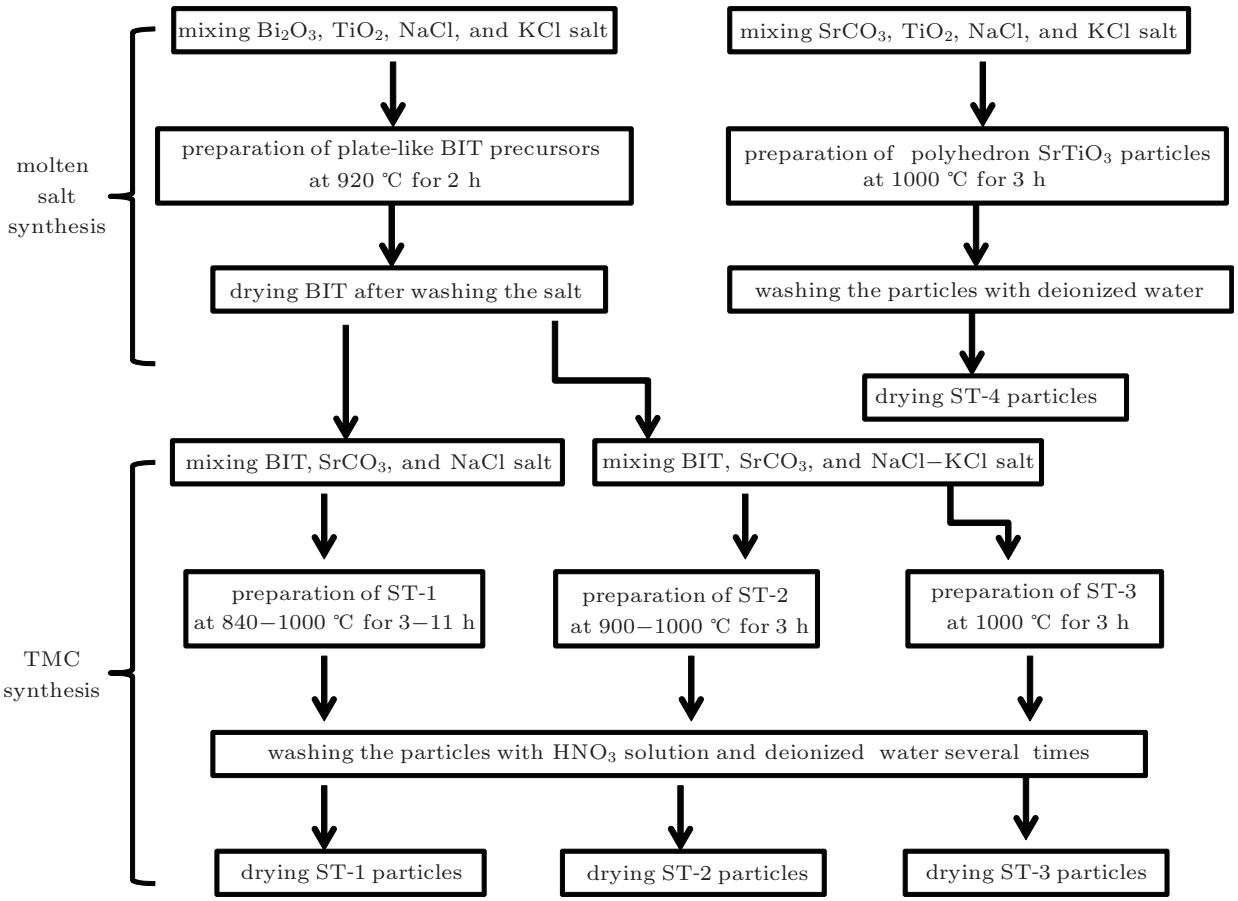


Fig. 1. Flow chart of preparing morphology-controlled $SrTiO_3$ particles.

2.3. Characterization

The XRD patterns of the samples were recorded by a Mini Flex II Desktop X-ray Diffractometer using Cu-K radiation ($\lambda = 1.54059$ Å) in the range $2\theta = 5°$–$85°$ in scan steps of 0.02°. The data analyses were carried out with the aid of the JADE 5.0 software package. Microstructures of all the samples were analyzed using a scanning electron microscope (SEM JSM-6700F).

3. Results and discussion

3.1. Plate-shape analysis of BIT precursors

The diffraction patterns of BIT particles obtained by a molten salt method are shown in Fig. 2. The predominant diffraction peak intensities of BIT samples obtained in NaCl flux (Fig. 2(b)) can be indexed to the phase of BIT (JCPDS-73-2181), although a few of the secondary phases are visible such as $Na_nTi_4O_8$ and TiO_2 phases. However, figure 2(a) indicates that the XRD patterns of BIT in NaCl–KCl complex flux are nicely indexed to an orthorhombic BIT phase, indicating that the obtained powder is a highly crystallized phase of pure $Bi_4Ti_3O_{12}$.

It can be seen from Fig. 2 that the degree of anisotropy for pure perovskite structure particles prepared at 920 °C simultaneously increases with the addition of KCl salt. First, the compounds are annealed at the flux molten point (m.p.) for an hour and then the temperature increases for a higher synthesis sintering. The molten points of NaCl, NaCl–KCl, and Bi_2O_3 are 801 °C, 657 °C, and 820 °C, respectively. It can be concluded that the molten points of NaCl and Bi_2O_3 are so close to each other that the sintering process around 800 °C acceler-

ates the volatilization of Bi_2O_3, which leads to the secondary phases such as $Na_nTi_4O_8$ and TiO_2. However, the NaCl–KCl complex salt has a much lower molten salt (657 °C). Furthermore, the complex salt has better liquidity than single NaCl salt, which is more advantageous in the synthesis of pure Bi-rich products.

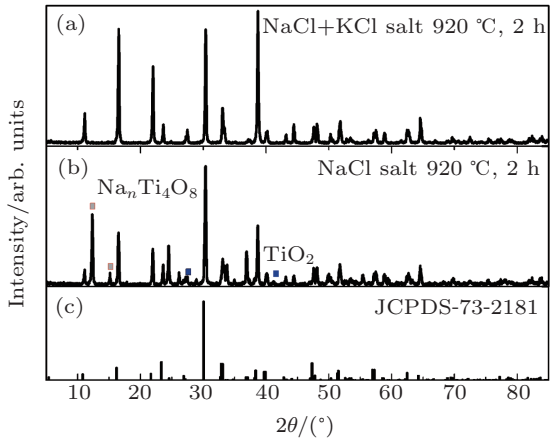


Fig. 2. XRD patterns of the prepared BIT powders (a) in NaCl and KCl compounds, (b) NaCl salt, and (c) the stand diffraction pattern of BIT (JCPDS-73-2181).

The scanning electron microscopy (SEM) image of BIT particles in NaCl–KCl salt is shown in Fig. 3. The particles always have constant plate properties with a mean size up to 0.3 μm×8 μm×8 μm synthesized at 920 °C for 2 hours. Thus, in this process, the plate-shaped BIT is obtained and provides sufficient precursors with large size and regular templates to build up $SrTiO_3$ plates with the perovskite structure.

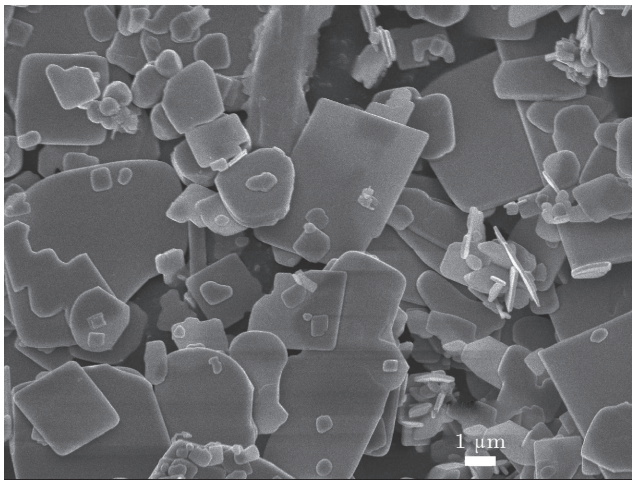


Fig. 3. SEM image of plate-shaped BIT precursors.

3.2. Morphology analysis of plate-like, reticular, and rod-like ST by ion-exchange, and cubic ST by the conventional molten salt method

For the plate-, reticula-, and rod-shaped products, we use $SrCO_3$ as the strontium precursors and BIT, with plate morphologies, as the titanium precursors. Our results indicate that different fluxes adopted in the same sintering process lead to various morphologies in the molten salt synthesis of $SrTO_3$.

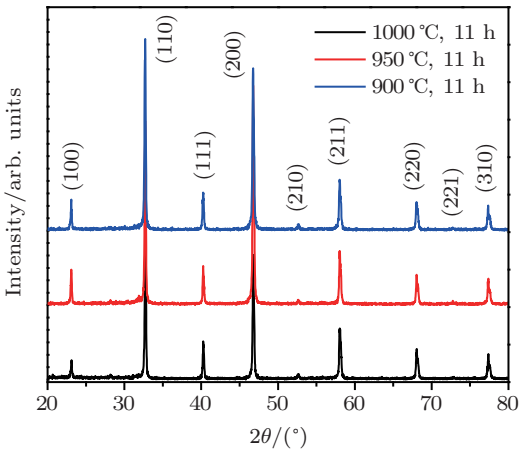


Fig. 4. (color online) XRD patterns of ST plates synthesized at 900 °C, 950 °C, and 1000 °C for 11 h and washed by nitric and diluting water.

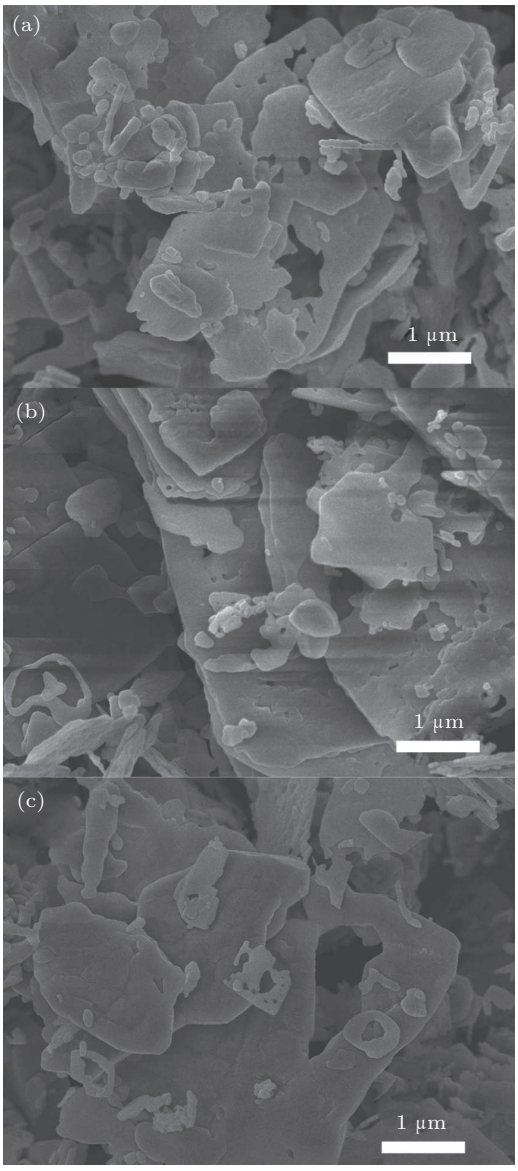


Fig. 5. SEM images of ST particles synthesized in molten salt at (a) 1000 °C, (b) 950 °C, and (c) 900 °C for 11 h.

Figure 4 displays the XRD patterns of ST plates synthesized in single NaCl salt from 900 °C–1000 °C for 11 h. All the diffraction peaks can be indexed to the cubic phase of ST (JCPDS 35-0734), indicating the prepared powder at 900 °C is a highly crystallized phase of pure $SrTiO_3$, above or below which the structure was still maintained. The SEM image (Fig. 5) demonstrates that the shape of the ST product is extremely related to that of the plate-like BIT precursor. However, the plates exhibit melting zones at these temperatures, and the particles are seriously hollowed at 1000 °C, leading to many holes through the plates, as shown in Fig. 5(a).

The holes in the particles indicate that the sintering temperature is too high for the synthesis of the plates, so the sintering temperature is reduced in the following experiments. Figures 6 and 7 display the XRD patterns and the effects of the sintering process on the morphology of ST particles at 840 °C–900 °C for 11 h, respectively. With temperature decreasing, the particles are first relatively hollowed and inhomogeneous but then become clean and uniform.

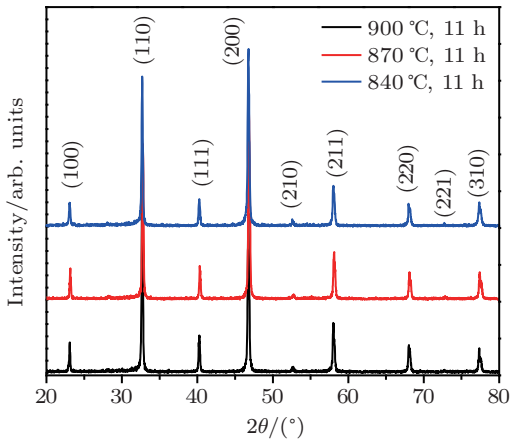


Fig. 6. (color online) XRD patterns of ST synthesized at 840 °C, 870 °C, and 900 °C for 11 h and washed by HNO_3 solution and diluting water.

To investigate the fabrication shape of ST plates at 840 °C, the raw materials are sintered at 840 °C but for different soaking times in NaCl salt. Figure 8 shows the XRD results of ST plates synthesized at 840 °C for 3 h–11 h, which verifies that there is no detectable impurity peak, and the effects of the soaking time in flux on ST particles are shown in Fig. 9. When the soaking time is reduced from 11 h to 7 h at 840 °C, the products display more anisotropic growth than at 840 °C for 11 h, but it is not uniform. When the sample was soaked at 840 °C for 3 h, the sizes of ST particles decrease and many irregular particles are found because of the low solubility and mobility of the oxides in NaCl salt at low temperature. It can be seen from Fig. 9 that the ST plates (ST-1) at 840 °C for 11 h exhibit the cleanest surface and large sizes (the mean size up to 0.2 μm×4 μm×4 μm) compared with the other samples when the soaking time is reduced.

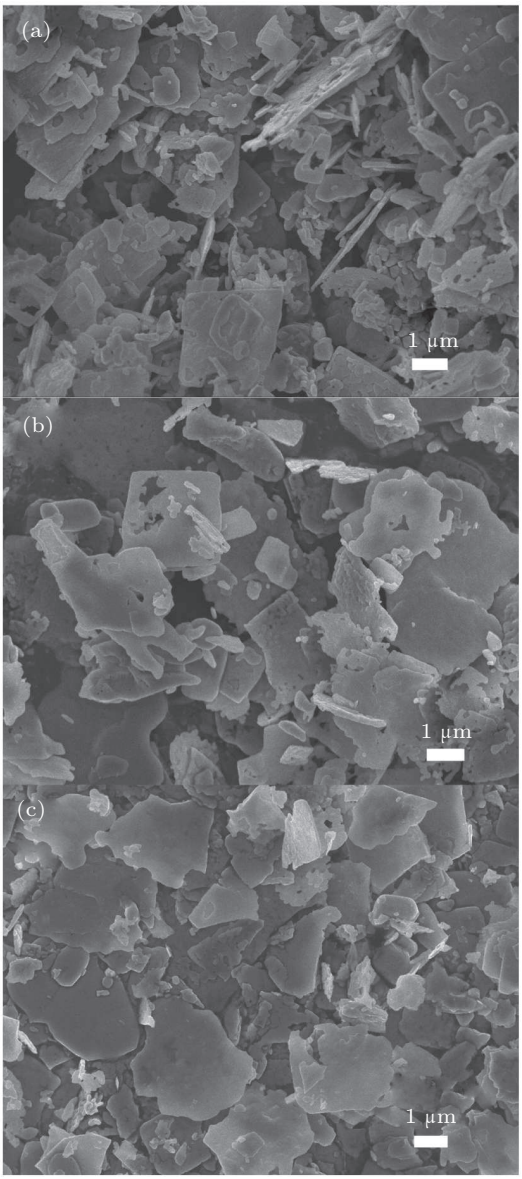


Fig. 7. SEM images of ST plates particles synthesized in molten salt at (a) 900 °C, (b) 870 °C, and (c) 840 °C for 11 h.

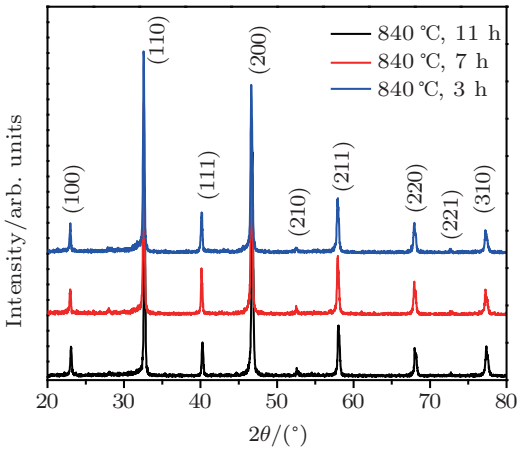


Fig. 8. (color online) XRD images of ST plates synthesized in NaCl salt at 840 °C for 3 h, 7 h, and 11 h.

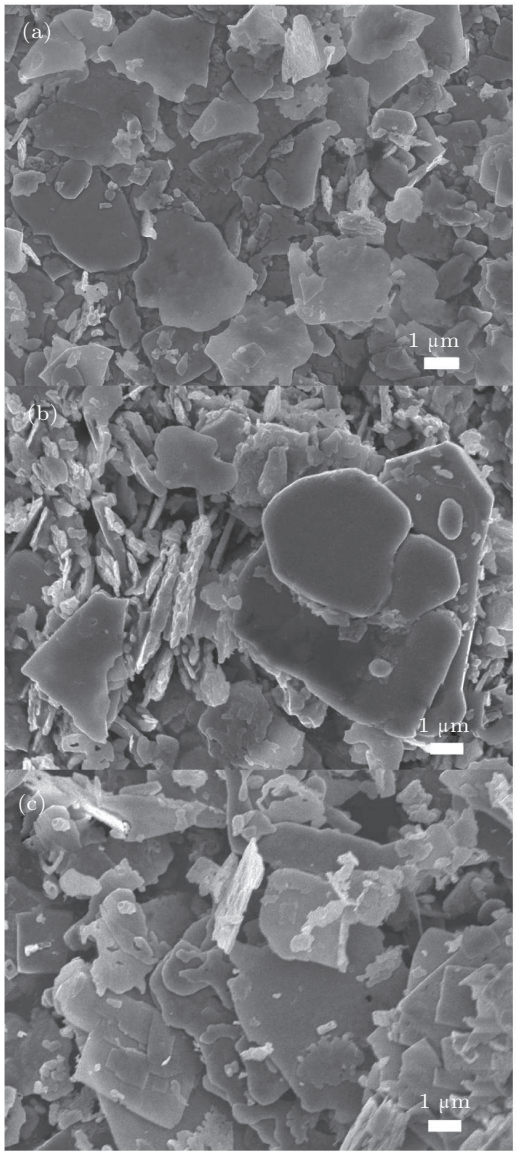


Fig. 9. SEM images of ST plates synthesized at 840 °C for (a) 11 h (ST-1), (b) 7 h, and (c) 3 h in NaCl salt.

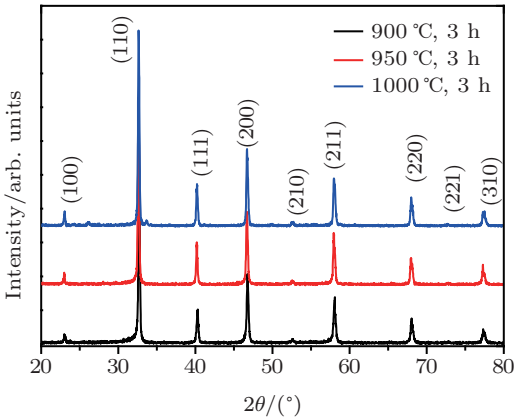


Fig. 10. (color online) XRD patterns of ST particles synthesized in NaCl–KCl salts at 900 °C, 950 °C, and 1000 °C for 3 h.

Further investigation is also made to study the growth features of ST particles when the synthesis process is changed. In order to analyze the characteristic influence of the flux, a half mole of NaCl is replaced by KCl in the ST plates synthesis by a two-step molten salt method. As shown in Fig. 10, the pure phase of ST can also be obtained in NaCl–KCl salt above 900 °C for 3 h. The ST plates can be synthesized in NaCl salt, however, the well-developed reticular ST particles are obtained when half NaCl is replaced by KCl in mole ratio for a comparative morphology, as shown in Fig. 11(a).

Figures 11(a) and 11(b) indicate that the products always maintain a reticula-shape fabricated from the BIT plates at temperatures in a range between 900 °C and 950 °C. When the temperature is increased from 950 °C (ST-2) to 1000 °C (ST-3) for 3 hours, the reticular ST-2 suddenly decreases and regular rod-shape particles form, as shown in Fig. 11(c). The further increase of sintering temperature does not obviously change the morphologies of ST products according to our experiments.

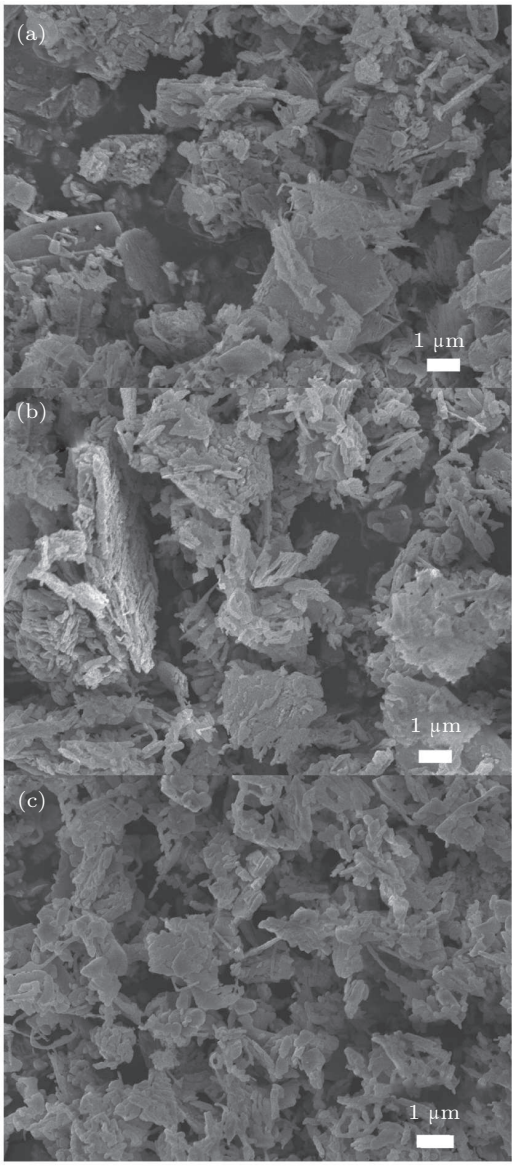


Fig. 11. SEM images of ST-2 (b) and ST-3 (c) particles synthesized at (a) 900 °C, (b) 950 °C, and (c) 1000 °C for 3 h.

To investigate the effect of the precursors on the ST morphology, the comparative experiments by different precursors (Fig. 12 for XRD pattern) are carried out. Herein ST-4 particles with a cubic morphology are sintered in the same amount of NaCl–KCl flux (1:4 in weight ratio, 50%-mol NaCl and 50%-mol KCl) with the raw materials $SrCO_3$ and TiO_2 as strontium and titanium precursors at 1000 °C for 3 h. It is noticed that the ST particles each exhibit a uniform cubic shape, which is much different from ST-3, as shown in Figs. 11(c) and 13(d). The experiments indicate that the morphology of ST can also be affected by changing the precursors.

Finally, the SEM photographs of the samples with different shapes in this research are shown in Fig. 13. It can be concluded that all the samples are different and the sintering process, the flux, and the precursors have significant influences on the morphology of ST, for the particles change significantly through changing the sintering temperature and soaking time, increasing the KCl flux and changing the strontium and titanium precursors.

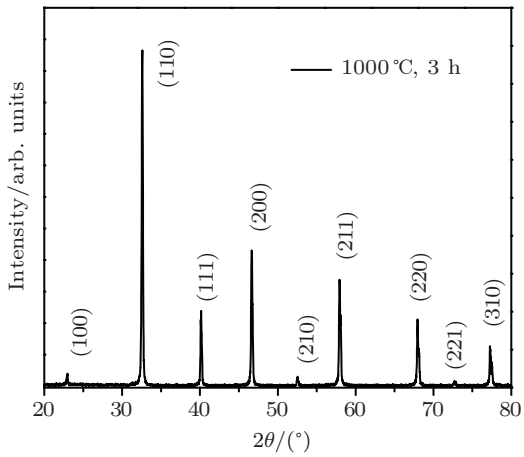


Fig. 12. XRD pattern of ST-4 particles synthesized at 1000 °C for 3 h.

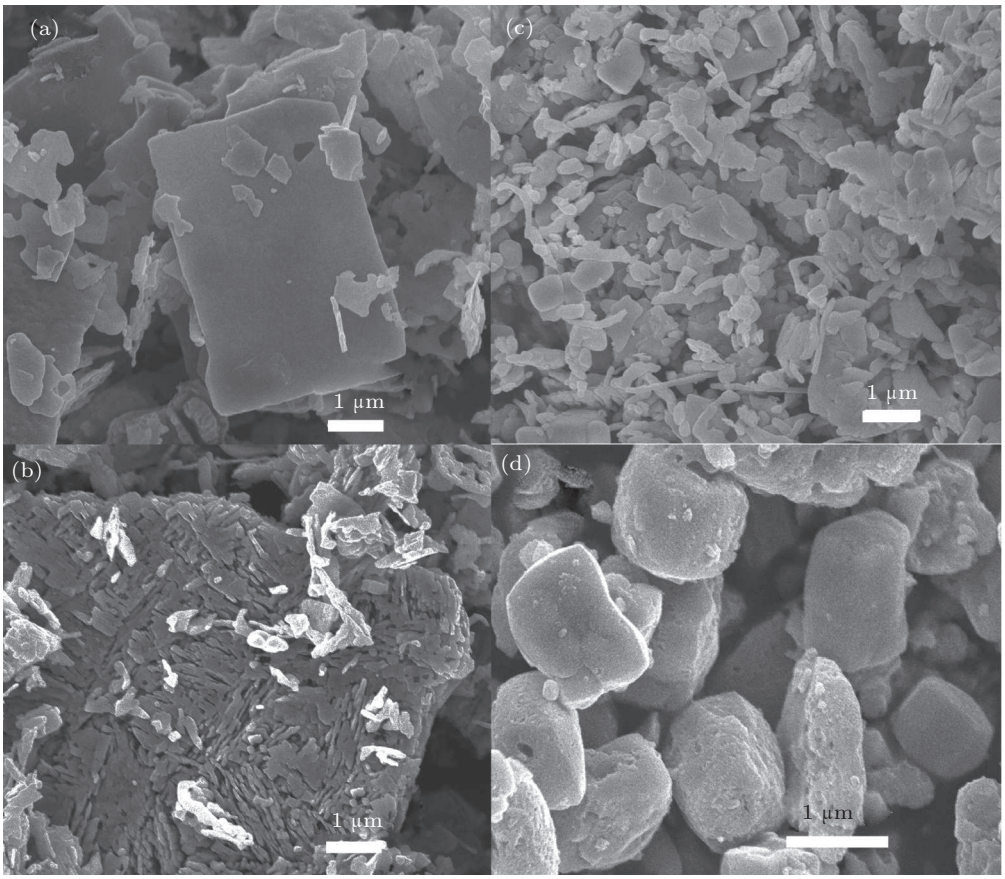


Fig. 13. SEM images of ST particles (a) ST-1, 840 °C for 11 h in NaCl salt, (b) ST-2, 950 °C for 3 h, (c) ST-3, 1000 °C for 3 h, and (d) ST-4, 1000 °C for 3 h in NaCl–KCl salt.

3.3. Crystalline analysis of ST particles under different conditions

The factors affecting the anisotropic growth of the final products include the precursors, the flux, and the sintering processes. First, the BIT plates can be maintained in NaCl single flux below 1000 °C, and the results show that the initial shape of the precursor can determine the final morphology, which is as important as the effects of the sintering process.

As shown in Fig. 14, for the synthesis by a two-step molten salt method, the Bi ions in the Bi_2O_2-layered struc-

ture may be first exchanged with Sr ions for the high activity of Bi in bismuth-layer structure Bi_2O_2-, then the increasing of the temperature causes a transposition between Bi ions in the perovskite structure and Sr ions. The mild melting solution built by NaCl salt can maintain the BIT plates and induce the formation of ST plates by ions exchange. However, the scheme will not performed under different flux conditions and sintering temperatures, just like the reticular-fabrication for ST-2 particles at 950 °C in NaCl–KCl salt for a better and destructive liquidity. Thus the NaCl–KCl flux at a lower eutectic point can break up the plates and induce new shape fabrication above 1000 °C such as rods for their better liquidity and low melting point (avoiding ions volatilization). As shown in Fig. 15, the layer structure is so seriously destroyed and disturbed that the well-evolved rod-shaped particles are obtained in the final products in NaCl–KCl flux at the same temperature.

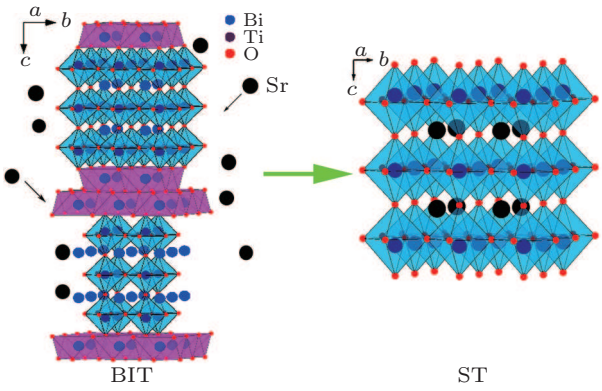


Fig. 14. (color online) Illustration view of the layered BIT precursors and ST plates, and schematic structure of plane transformation from BIT to ST plates.

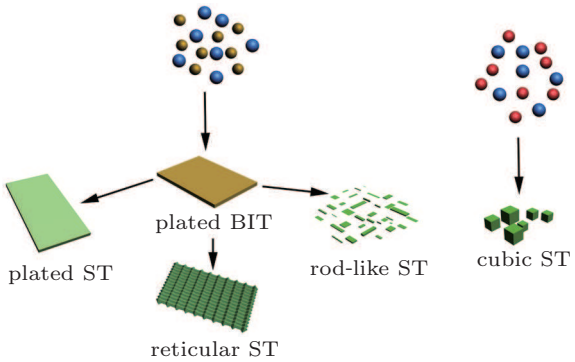


Fig. 15. (color online) Proposed schematic diagram of the synthetic mechanism of ST-1, ST-2, ST-3, and ST-4 particles in the molten salt.

Furthermore, the shapes of ST can be critically determined by changing the sintering temperature and soaking time. The microcrystal can nucleate and grow up into various shapes through mass transportation in liquid phase under different conditions. Thus the precursors, the flux, and the sintering process can be used to control the shape and size of the final products. All in all, this research provides a novel approach to fabricating morphology-controlled micro-scale ST particles with perovskite structure.

4. Conclusions

In the present study, we develop a simple and novel synthetic process of $SrTiO_3$ (ST) by changing the molten salt conditions such as the flux, the precursors, the sintering temperature, and soaking time, for designing morphology-controlled $SrTiO_3$ micro-scale crystals. The morphology of the plate-like BIT precursor is retained during the ion-exchanges into ST plates in NaCl salt below 1000 °C. However, particular attention is paid to the flux effect on the morphologies of ST particles in view of reticular and rod-shaped ST when the half mole ratio of NaCl is replaced by KCl. We also report that the precursors can affect the shape of ST, for the cubic ST is obtained by changing the strontium and titanium precursors in the same sintering condition. The results demonstrate the internal synthetic mechanism for the $SrTiO_3$ micro-scale crystals and may provide guidance for the shape-controlled synthesis of materials with a perovskite structure.

Acknowledgment

The authors are grateful to the School of Mathematics and Physics, Anhui University of Technology for support.

References

[1] Petrov P K, Ivanov Z G and Gevorgyan S S 2000 *Mater. Sci. Eng. A* **288** 231
[2] Hu Y, Tan O K, Pan J S and Yao X 2004 *J. Phys. Chem. B* **108** 11214
[3] Konta R, Ishii T, Kato H, Kudo H and Kudo A 2004 *J. Phys. Chem. B* **108** 8992
[4] Kan D, Terashima T, Kanda R, Masuno A, Tanaka K, Chu S H, Kan H F, Ishizumi A, Kanemitsu Y, Shimakawa Y C and Takano M 2005 *Nat. Mater.* **4** 816
[5] Wang Q Y, Li Z, Zhang W H, Zhang Z C, Zhang J S, Li W, Ding H, Ou Y B, Deng P, Chang K, Wen J, Song C L, He K, Jia J F, Ji S H, Wang Y Y, Wang L L, Chen X, Ma X C and Xue Q K 2012 *Chin. Phys. Lett.* **29** 037402
[6] Ohno T, Tsubota T, Nakamura Y and Sayama K 2005 *Appl. Catal. A: Gen.* **288** 74
[7] Miyauchi M, Takashio M and Tobimatsu H 2004 *Langmuir* **20** 232
[8] Domen K, Kudo A, Onishi T, Kosugi N and Kuroda H 1986 *J. Phys. Chem.* **90** 292
[9] Kumar A, Santangelo P G and Lewis N S 1992 *J. Phys. Chem.* **96** 834
[10] Wrighton M S, Ellis A B, Wolczanski P T, Morse D L, Abrahamson H B and Ginley D S 1976 *J. Am. Chem. Soc.* **98** 2774
[11] Puangpetch T, Sreethawong T, Yoshikawa S and Chavadej S 2008 *J. Mol. Catal. A: Chem.* **287** 70
[12] Liu Y, Xie L, Li Y, Yang R, Qu J L, Li Y Q and Li X G 2008 *J. Power Sources* **183** 701
[13] Usimaki A, Vahakangs J and Leppavuori S 1982 *J. Am. Ceram. Soc.* **65** 147

[14] Tang D S, Zhou W Y, Ci L J, Yan X Q, Yuan H J, Zhou Z P, Liang Y X, Liu D F and Liu W 2002 *Chin. Phys.* **11** 496
[15] Tian B L, Du Z L, Ma Y M, Li X F, Cui Q L, Cui T, Liu B B and Zou G T 2010 *Chin. Phys. Lett.* **27** 026103
[16] Souza A E, Santos G T A, Barra B C, Macedo W D, Teixeira S R, Santos C M, Senos A M R, Amaral L and Longo E 2012 *Cryst. Growth Des.* **12** 5671
[17] Liu Q L, Yu G H and Jiang Y 2009 *Chin. Phys. B* **18** 1266
[18] Muhamad S F, Zubair A and Khaulah S 2012 *Chin. Phys. Lett.* **29** 126802
[19] Bockrath M, Liang W, Bozovic D, Hafner J H, Lieber C M, Tinkham M and Park H 2001 *Science* **291** 283
[20] Liang W J, Bockrath M, Bozovic D, Hafner J H, Tinkham M and Park H 2001 *Nature* **411** 665
[21] Thurn-Albrecht T, Schotter J, Kästle G A, Emley N, Shibauchi T, Krusin-Elbaum L, Guarini K, Black C T, Tuominen M T and Russell T P 2000 *Science* **290** 2126
[22] Huang M H, Mao S, Feick H, Yan H Q, Wu Y Y, Kind H, Weber E, Russo R and Yang P D 2001 *Science* **292** 1897
[23] Dong W J, Li X Y, Yu J, Guo W C, Li B J, Tan L, Li C R, Shi J J and Wang G 2012 *Mater. Lett.* **67** 131
[24] Fu Q, He T, Li J L and Yang G W 2012 *J. Appl. Phys.* **112** 104322
[25] Saito Y, Takao H, Tani T, Nonoyama T, Takatori K, Homma T, Nagaya T and Nakamura M 2004 *Nature* **432** 84
[26] Saito Y and Takao H 2007 *J. Eur. Ceram. Soc.* **27** 4085
[27] Zhao W, Zhou H P, Yan Y K and Liu D 2008 *J. Am. Ceram. Soc.* **91** 1322